

Synthesis and Magnetic Properties of Iron Nanoellipsoids Bioinspired by Magnetotactic Bacteria

Carlos Luna^{1,a}, Enrique D. Barriga-Castro^{1,b}
and Raquel Mendoza-Reséndez^{2,c}

¹Centro de Investigación en Ciencias Físico Matemáticas (CICFiM) / Facultad de Ciencias Físico Matemáticas (FCFM), Universidad Autónoma de Nuevo León (UANL), Av. Universidad S/N, San Nicolás de los Garza, Nuevo León 66450, Mexico. ²Facultad de Ingeniería Mecánica y Eléctrica (FIME), Universidad Autónoma de Nuevo León (UANL), Av. Universidad S/N, San Nicolás de los Garza, Nuevo León 66450, Mexico.

^acarlos.lunacd@uanl.edu.mx, ^be.diazb776@hotmail.com, ^craquel.mendozars@uanl.edu.mx

Keywords: Nanoellipsoids, Magnetic Nanoparticles, Chain of Spheres Model, Magnetic Anisotropy

Abstract. Ferromagnetic iron nanoellipsoids were prepared by the hydrogen reduction of ellipsoidal hematite nanoarchitectures. These magnetic nanoscale particles displayed a microstructure that showed clear similarities to the magnetosome chains of the magnetotactic bacteria. Specifically, such nanoellipsoids are formed by single-domain nanocrystals assembled into double chains sharing the same crystallographic orientation. In the present contribution, the magnetic properties of the Fe nanoellipsoids were explained considering the chain of spheres model of Jacobs and Bean, and thermal effects.

Introduction

The reduction of the material dimensions into the nanoscale implies the appearance of new physical properties and behaviors arising from surface, interface, confinement and interparticle interaction effects, which have negligible contributions in bulk materials. Therefore, a fundamental and exciting challenge of modern material sciences is to develop new routes that allow the growth of low dimensional systems, obtaining 2D systems (thin films), 1D nanostructures (nanowires, nanotubes, nanobelts, nanochains, etc.) and 0D materials (nanoparticles and quantum dots), respectively.

Many methods have been developed for preparing materials with tailored dimensionalities and with different physical behaviors [1-12]. However, it is noteworthy that, until recently, investigations of magnetic 1D nanostructures have advanced relatively little in comparison with other low-dimensional systems, mainly because magnetic materials usually present isotropic growth habits. Thus, there are relatively few preparation techniques of magnetic nanostructures with anisotropic morphologies [8-12]. One of the most used methods involves the chemical reduction of iron oxide nanoparticles with spindle-like or rod-like morphologies [13-16]. Recently, we have proposed new strategies of synthesis based on the hydrogen reduction of hematite ellipsoidal nanoarchitectures to obtain magnetic nanoellipsoids (NEs) with engineered microstructures formed by chains of single-magnetic domain crystals sharing the same crystallographic orientation, and exhibiting certain similarities to the magnetosome chains of the magnetotactic bacteria [16]. In the present contribution we described the magnetization reversal process of these NEs using the chain of spheres model of Jacobs and Bean, and considering the effects of thermal fluctuations.

Experimental Techniques

Preparation of the Samples. Iron nanoellipsoids were prepared using the method described in detail elsewhere [14-17]. In brief, initial hematite elongated nanoparticles were prepared by the forced hydrolysis of aqueous solutions of 0.1 M iron (III) perchlorate ($\text{Fe}(\text{ClO}_4)_3$, Fluka, >98%), 4.5 mM sodium dihydrogen phosphate (NaH_2PO_4 , Fluka, >97%) and 0.1 M urea (Merck, >99%) at 100°C during 48 hours. The precipitated solid was separated from the solution by centrifugation and it was washed several times with doubly distilled water. Afterwards, the hematite nanoparticles were reduced to α -Fe nanoellipsoids under a hydrogen flow of 40 l/h for 4 h at 400°C. Finally, a N_2

gas wetted with ethanol was passed through the sample in order to passivate the surface of the Fe NEs.

Characterization techniques. The X-ray diffraction (XRD) pattern of the iron NEs was measured using a Siemens D5000 diffractometer with Cu K α radiation ($\lambda = 1.5418 \text{ \AA}$). The mean length of the crystalline domains, L , associated to the more intense diffraction peak was estimated from the full width at half maximum (FWHM) using the Scherrer equation [18]. The particle size and morphology of the NEs were examined by transmission electron microscopy (TEM) using a FEI-TITAN 80-300 kV microscope operating with an accelerating voltage of 300 kV. For TEM analysis, the NEs were suspended in water and deposited onto lacey carbon copper grids. Also, selected area electron diffraction (SAED) patterns were measured. The magnetic characterization was carried out with the sample in form of compacted powder and using a commercial vibrating sample magnetometer VSM (Quantum Design).

Results and Discussion

Fig. 1a shows the XRD pattern of the iron NEs in the 2θ range from 20 to 70°. In this pattern well-defined and very intense diffraction peaks are observed at around 44.84 and 65.27°, which can be indexed to the (110) and (200) reflections of the body centered cubic (bcc) crystal structure of α -iron (space group Im3m). The mean length L perpendicular to the (110) planes calculated using equation (1) was 28.8(3) nm. The XRD results were corroborated by SAED pattern analysis, where several spotty rings associated to the (110), (200), (211), (310) and (400) planes of the bcc α -Fe were clearly observed (see the inset image of Fig. 1c).

Fig. 1c depicts a representative TEM micrograph of the Fe NEs. In this image, uniform elongated particles with an average width of 45(3) nm and an average length of 210(18) nm are observed. High-magnification TEM images (Fig. 1d) revealed that the Fe NEs are formed by sub-units of around 25 nm (i.e. a size close to the estimated mean length L perpendicular to the (110) planes). These sub-units appear in the TEM image coated by a very thin surface layer corresponding to the oxide surface layer formed during the controlled passivation process. On the other hand, these sizes are of the same order than the critical diameter for single domain behavior of Fe [17], thus the observed sub-units should be magnetic single-domain nanocrystals. In addition, detailed studies carried out elsewhere [17] showed that these assembled nanocrystals share the same crystalline orientation, exhibiting an arrangement similar than that observed in the magnetosomes of the magnetotactic bacteria [19].

Given the particular microstructure of the NEs, these nanoparticles can be used as suitable experimental models for the study of the magnetization reversal processes that can occur in linear chains of magnetic single-domain nanocrystals, and specifically to test the *chain-of-spheres model* of Jacobs and Bean [20]. This micromagnetic model predicts the corresponding coercive field values of linear chains of single-domain spheres assuming different magnetization reversal mechanisms. In this model, only magnetostatic interactions among the spheres are considered, and the effects of the interactions between the chains of spheres, the thermal agitation and the magnetocrystalline anisotropy are not considered. The two main magnetization reversal mechanisms considered by this model are the parallel rotation of the magnetic moments of the single-domain spheres and the symmetric fanning mechanisms [20]. For the parallel rotation mechanism, the coercive field of a linear chain with n spheres when the magnetic field direction is aligned along the chain axis is given by:

$$H_c = \pi K_n M_s \quad (1)$$

whereas for the symmetric fanning mechanism, the coercive field is given by:

$$H_c = \frac{\pi M_s}{6} (6K_n - 4L_n) \quad (2)$$

where

$$L_n = \sum_{i=1}^{\frac{n-1}{2} < i \leq \frac{n+1}{2}} \frac{n - (2i - 1)}{n(2i - 1)^3}, \quad M_n = \sum_{i=1}^{\frac{n-2}{2} < i \leq \frac{n}{2}} \frac{n - 2i}{n(2i)^3}, \quad K_n = L_n + M_n = \sum_{i=1}^n \frac{n - i}{ni^3} \quad (3)$$

For randomly oriented chains, the coercive field values associated to these mechanisms are 47.9% and 110% of the estimated value for chains aligned along the direction of the applied field [20], respectively.

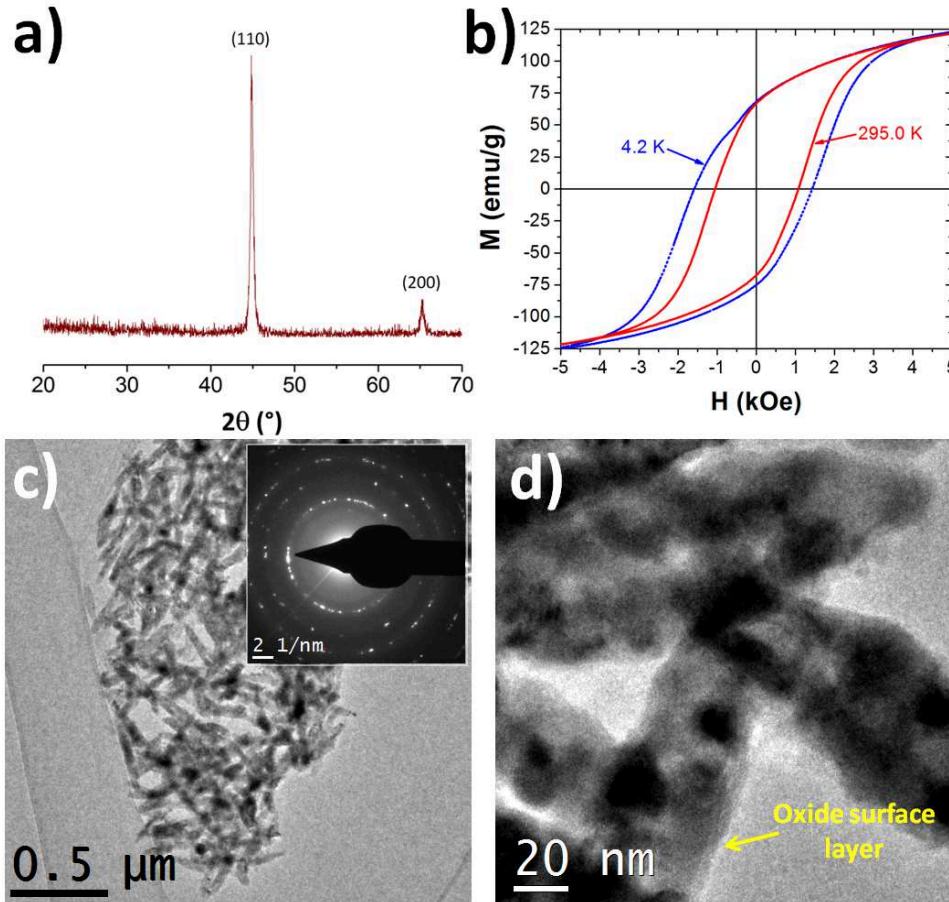


Fig. 1 a) XRD diffraction pattern of α -Fe nanoellipsoids. b) Hysteresis loops of the α -Fe NEs measured at 4.2 and 295 K. c) Typical TEM image of the iron nanoellipsoids. The inset shows a SAED pattern. d) High-magnification TEM micrograph of the Fe NEs.

Fig. 1b shows the magnetic hysteresis loops of the NEs in form of compacted powder (therefore, it is expected that the NEs are randomly oriented) measured at 4.2 and 295 K. The coercive field found at 295 K was 1,065 Oe. This value is about twice that of the maximum coercivity for a single domain α -Fe particle with a predominant magnetocrystalline anisotropy ($H_C = 2K_1/M_S \approx 560$ Oe, where $K_1 = 4.8 \times 10^5$ erg/cm³ is the anisotropy constant [21]). On the other hand, this value is also significantly higher than the values experimentally observed in equiaxial iron nanoparticles with diameters around 30 nm at room temperature [22]. These facts indicate that the shape anisotropy is the main source of magnetic anisotropy in the NEs studied herein. Assuming $n = 6$, the experimental value of the saturation magnetization ($M_S \approx 150$ emu/g) and a random orientation of the chains, the values of H_C predicted by the chain-of-spheres model assuming the parallel rotation and the symmetric fanning mechanisms are 1,671 and 1,520 Oe, respectively. The significant difference between these values and the experimental value measured at 295 K are mainly due to effects of thermal agitation and maybe to interparticle interactions, which should lead to the reduction of the coercivity of the nanoellipsoid system [17, 23]. In order to reduce the thermal effects, the hysteresis loop of the nanoellipsoids was measured at 4.5 K (Fig. 1b). The coercive field

obtained under these conditions ($H_C = 1,508$ Oe) was the 90 and 99 % of the values calculated considering the above two mechanisms of magnetization reversal, respectively. Therefore, this model reasonably predicts the coercive field of the nanoellipsoids when the thermal effects are minimized, suggesting that the interparticle interaction effects don't display an important contribution in the magnetic behavior of this particle system when the nanoellipsoids are randomly oriented. Nevertheless, it is important to note that the increment of the coercivity of the NEs as the temperature decreases could partially be due to the induction of an exchange coupling between the oxide surface layer and the iron sub-units at low temperature [23], and this enhancement of the coercive field is not considered in the chain-of-spheres model.

Conclusions

Stabilized Fe NEs bioinspired by magnetotactic bacteria can be successfully prepared through the hydrogen reduction of hematite ellipsoidal particles. The resulting Fe NEs exhibit a microstructure constituted by single-domain subunits aligned in two chains. The study of the magnetic properties of these nanoscale system showed that the predominant source of the magnetic anisotropy is the shape anisotropy, and they can be satisfactorily predicted with the chain of spheres model assuming a symmetric fanning mechanism for magnetization reversal when the thermal agitation effects are minimized.

Acknowledgements

Financial support from the Mexican Council of Science and Technology (CONACYT) and Universidad Autónoma de Nuevo León under research projects CB-179486 and PAICYT-CE793-11, respectively, is acknowledged.

References

- [1] M. Brust, M. Walker, D. Bethell, D.J. Schiffrin, R. Whyman: *J. Chem. Soc., Chem. Commun.* Vol. 7 (1994), p. 801.
- [2] M. Ohring: *Materials science of thin films* (Academic press., USA 2001).
- [3] C. Luna, C.J. Serna, M. Vázquez: *Nanotechnology* Vol. 15 (2004), p.S293.
- [4] A.H. Lu, E.E. Salabas, F. Schüth: *Angewandte Chemie International Edition* Vol. 46 (2007), p. 1222.
- [5] B. Folch, J. Larionova, Y. Guari, K. Molvinger, C. Luna, C. Sangregorio, C. Innocenti, A. Caneschi, C. Guérin: *Physical Chemistry Chemical Physics* Vol. 12 (2010), p.12760.
- [6] R. Mendoza-Reséndez, A. Gómez-Treviño, E. D. Barriga-Castro, N. O. Núñez, C. Luna: *RSC Advances* Vol. 4 (2014), p. 1650.
- [7] C. Luna, E.D. Barriga-Castro, R. Mendoza-Reséndez: *Acta Materialia* Vol. 66 (2014), P. 405.
- [8] T. Mårtensson, P. Carlberg, M. Borgström, L. Montelius, W. Seifert, L. Samuelson: *Nano Letters* Vol. 4 (2004), p. 699.
- [9] L.J. Guo: *Advanced Materials* Vol. 19 (2007), p. 495.
- [10] C. Luna, M. Ilyn, V. Vega, V. M. Prida, J. González, R. Mendoza-Reséndez: *The Journal of Physical Chemistry C* Vol. 118 (2014), p. 21128.
- [11] J. Martín, M. Hernández-Vélez, O. de Abril, C. Luna, A. Muñoz-Martin, M. Vázquez, C. Mijangos: *European Polymer Journal* Vol. 48 (2012), p.712.
- [12] V.M. Prida, J. García, L. Iglesias, V. Vega, D. Görlitz, K. Nielsch, E.D. Barriga-Castro, R. Mendoza-Reséndez, A. Ponce, C. Luna: *Nanoscale research letters* Vol. 8 (2013), p. 263.
- [13] N.O. Nuñez, P. Tartaj, M.P. Morales, R. Pozas, M. Ocaña, C.J. Serna: *Chem. Mater.* Vol 15 (2003), p. 3558.
- [14] R. Mendoza-Reséndez, M. P. Morales, C. J. Serna. *Mater. Sci. Eng. C* vol. 23 (2003), p. 1139.
- [15] R. Mendoza-Reséndez, O. Bomati-Miguel, M.P. Morales, P. Bonville, C.J. Serna: *Nanotechnology* Vol. 15, 2004, p. S254.
- [16] R. Mendoza-Reséndez, R. Pozas, M.P. Morales, P. Bonville, M. Ocaña, C.J. Serna: *Nanotechnology* Vol 16 (2005), p. 647.

-
- [17] R. Mendoza-Reséndez, C. Luna, E.D. Barriga-Castro, P. Bonville, C.J. Serna: *Nanotechnology* Vol. 23 (2012), p. 225601.
- [18] B.D. Cullity, S.R. Stock: *Elements of X-ray Diffraction* (Prentice-Hall, New York, USA 2001).
- [19] R.E. Dunin-Borkowski, M.R. McCartney, R.B. Frankel, D.A. Bazylinski, M. Pósfai, P.R. Buseck: *Science* Vol. 282 (1998), p. 1868.
- [20] I.S. Jacobs, C.P. Bean: *Phys. Rev.* Vol 100 (1955), p. 1060.
- [21] S. Chikazumi: *Physics of Magnetism* (Wiley, New York, USA 1964).
- [22] R. Fernández-Pacheco, M. Arruebo, C. Marquina, R. Ibarra, J. Arbiol, J. Santamaría: *Nanotechnology* Vol. 17 (2006), p. 1188.
- [23] R. Mendoza-Reséndez, C. Luna: *Journal of nanoscience and nanotechnology* Vol. 12 (2012), p. 7577.

Proceedings of the 4th International Conference on Materials and Applications for Sensors and Transducers

10.4028/www.scientific.net/KEM.644

Synthesis and Magnetic Properties of Iron Nanoellipsoids Bioinspired by Magnetotactic Bacteria

10.4028/www.scientific.net/KEM.644.35

DOI References

[1] M. Brust, M. Walker, D. Bethell, D.J. Schiffrin, R. Whyman: J. Chem. Soc., Chem. Commun. Vol. 7 (1994), p.801.

<http://dx.doi.org/10.1039/c39940000801>

[3] C. Luna, C.J. Serna, M. Vázquez: Nanotechnology Vol. 15 (2004), p. S293.

<http://dx.doi.org/10.1088/0957-4484/15/4/033>

[4] A.H. Lu, E.E. Salabas, F. Schüth: Angewandte Chemie International Edition Vol. 46 (2007), p.1222.

<http://dx.doi.org/10.1002/anie.200602866>

[5] B. Folch, J. Larionova, Y. Guari, K. Molvinger, C. Luna, C. Sangregorio, C. Innocenti, A. Caneschi, C. Guérin: Physical Chemistry Chemical Physics Vol. 12 (2010), p.12760.

<http://dx.doi.org/10.1039/c002432e>

[7] C. Luna, E.D. Barriga-Castro, R. Mendoza-Reséndez: Acta Materialia Vol. 66 (2014), P. 405.

<http://dx.doi.org/10.1016/j.actamat.2013.11.032>

[8] T. Mårtensson, P. Carlberg, M. Borgström, L. Montelius, W. Seifert, L. Samuelson: Nano Letters Vol. 4 (2004), p.699.

<http://dx.doi.org/10.1021/nl035100s>

[9] L.J. Guo: Advanced Materials Vol. 19 (2007), p.495.

<http://dx.doi.org/10.1002/adma.200600882>

[10] C. Luna, M. Ilyn, V. Vega, V. M. Prida, J. González, R. Mendoza-Reséndez: The Journal of Physical Chemistry C Vol. 118 (2014), p.21128.

<http://dx.doi.org/10.1021/jp5048634>

[12] V.M. Prida, J. García, L. Iglesias, V. Vega, D. Görlitz, K. Nielsch, E.D. Barriga-Castro, R. Mendoza-Reséndez, A. Ponce, C. Luna: Nanoscale research letters Vol. 8 (2013), p.263.

<http://dx.doi.org/10.1186/1556-276X-8-263>

[14] R. Mendoza-Reséndez, M. P. Morales, C. J. Serna. Mater. Sci. Eng. C vol. 23 (2003), p.1139.

<http://dx.doi.org/10.1016/j.msec.2003.09.126>

[15] R. Mendoza-Reséndez, O. Bomati-Miguel, M.P. Morales, P. Bonville, C.J. Serna: Nanotechnology Vol. 15, 2004, p. S254.

<http://dx.doi.org/10.1088/0957-4484/15/4/026>

[17] R. Mendoza-Reséndez, C. Luna, E.D. Barriga-Castro, P. Bonville, C.J. Serna: Nanotechnology Vol. 23 (2012), p.225601.

<http://dx.doi.org/10.1088/0957-4484/23/22/225601>

[19] R.E. Dunin-Borkowski, M.R. McCartney, R.B. Frankel, D.A. Bazylinski, M. Pósfai, P.R. Buseck: Science Vol. 282 (1998), p.1868.

<http://dx.doi.org/10.1126/science.282.5395.1868>

[20] I.S. Jacobs, C.P. Bean: Phys. Rev. Vol 100 (1955), p.1060.

<http://dx.doi.org/10.1103/PhysRev.100.1060>

[22] R. Fernández-Pacheco, M. Arruebo, C. Marquina, R. Ibarra, J. Arbiol, J. Santamaría: Nanotechnology

Vol. 17 (2006), p.1188.

<http://dx.doi.org/10.1088/0957-4484/17/5/004>

[23] R. Mendoza-Reséndez, C. Luna: Journal of nanoscience and nanotechnology Vol. 12 (2012), p.7577.

<http://dx.doi.org/10.1166/jnn.2012.6536>